Confinement properties of GFRP-RC circular c-bent columns under simulated seismic loading

Yasser M. Selmy[1], Amr E. Abdallah[2], Ehab F. El-Salakawy[3]

[1] PhD Candidate, Department of Civil Engineering, University of Manitoba, Winnipeg, Manitoba, Canada; Assistant Lecturer, Civil Engineering Department, Suez-Canal University, Ismailia, Egypt.
E-mail: selmyy@myumanitoba.ca
[2] Lecturer, Civil Engineering Department, Assiut University, Assiut, Egypt.
E-mail: abdalla3@myumanitoba.ca
[3] Professor, Department of Civil Engineering, University of Manitoba, Winnipeg, Manitoba, Canada.
E-mail: Ehab.El-Salakawy@umanitoba.ca

ABSTRACT

The current seismic design provisions for confinement reinforcement in fiber-reinforced polymer-reinforced concrete (FRP-RC) columns are overly conservative. One reason for that is the scarcity of research data. Despite the recent efforts to assess the confinement behavior in FRP-RC columns under simulated seismic loading, the effect of combined loading schemes incorporating torsion (e.g., C-bent bridge piers) is not experimentally addressed. This study investigates the behavior of three glass FRP (GFRP)-RC circular columns under earthquake-simulated loading including torsional effects. Two columns were confined by a GFRP spiral while discrete GFRP hoops were utilized to confine the other column. A sophisticated test setup was used to apply simultaneous axial loading and lateral drift reversals at a transverse eccentricity resulting in cyclic torque in addition to the shear and flexure load effects. While GFRP hoops with a lap splice equal to 60 times its cross-sectional diameter resulted in comparable behavior to spiral-confined GFRP-RC column when no torsional effects were present, better behavior was observed in this study for the GFRP-RC C-bent columns confined with spirals.

Keywords: Glass fiber-reinforced polymer (GFRP), Torsion, Seismic, Confinement, Spiral, Hoops.

INTRODUCTION

Due to the well-established detrimental effects of corrosion of steel reinforcement on the performance of steel-reinforced concrete (RC) structures in North America, the use of the non-corroding fiber-reinforced polymer (FRP) reinforcement, instead of conventional steel, is becoming a commonplace. This, in turn, requires the development of independent design provisions for FRP-RC structures due to the differences between the behavior of the two types of reinforcement. These differences include, but are not limited to, the linear elastic behavior of FRP up to failure, with relatively lower elastic modulus and without exhibiting any yielding. The latter attribute, in particular, imposed significant concerns about the use of FRP in seismic-force resisting systems (SFRSs), which was later rebutted by recent research [1-6]. For that reason, more detailed design provisions are available in the current design codes for FRP-RC structures [7-9] for particular elements such as flat plates, slabs and beams. On the other hand, the development of design provisions for other elements, such as columns, is still lagging behind due to the scarcity of research data.
While a significant amount of research was dedicated to the investigation of seismic behavior of FRP-RC columns in the last two decades [1-3, 6, 10-16], an important aspect such as the influence of cyclic torsion is still unexplored. A clear example of such case is the concept of C-bent columns, which can be used in bridges where a ground obstacle (such as traffic) forces an asymmetric alignment for the bridge pier, as shown in Fig. 1.

Fig. 1: An example of a C-bent column to allow pedestrian access

Previous research on steel-RC columns under simulated seismic loading including torsional effects reported earlier spalling of concrete cover, more extensive damage and lower lateral load and drift capacities compared to their counterparts that are experiencing no torsion [17-22]. While the current design codes for FRP-RC structures allow the use of confinement reinforcement in columns in the form of spirals or discrete hoops [7-9], the available literature on steel-RC columns under combined seismic loading schemes including torsion reported more severe core degradation for hoop-confined columns compared to those confined with spirals [23].
This paper investigates the behavior of three glass FRP (GFRP)-RC circular columns under simulated seismic loading incorporating cyclic torsion. In addition, the effect of transverse reinforcement configuration (i.e., spiral versus hoops) was evaluated in this study. The choice of GFRP was due to its relatively low cost and adequate strain capacity. The results of this study will introduce early insights into the behavior of such crucial elements in the RC infrastructure industry.

EXPERIMENTAL PROGRAM

Materials

All specimens were cast using a ready mixed, normal-weight concrete with a target 28-day compressive strength of 35 MPa. The actual compressive strength was determined for each specimen by testing standard 100 × 200-mm cylinders as per CSA A23.1-19/A23.2-19 [24] on the day of testing for each column, as summarized in Table 1. The longitudinal and transverse reinforcement for all columns was provided using sand-coated GFRP size No. 16 (i.e., 15.9-mm diameter) bars and size No. 10 (9.5-mm diameter) spirals or hoops, respectively. The physical and mechanical properties of the utilized GFRP bars, spirals and hoops, as provided in the certificate of compliance issued by the manufacturer [25] or as determined by laboratory testing [8], as appropriate, are listed in Table 2.

Table 1: Properties of the test specimens

Specimen ID	Torsion-to-bending moment, t_m	Cracking load applied kN	Concrete strength, f_c' MPa	Transverse reinforcement type	Average length of hinging region, L_i mm
G-0-S	0	20	38.8 ± 0.9	Spiral	450
G-0.2-S	0.2	25	44.1 ± 0.9	Spiral	530
G-0.2-H	0.2	25	40.7± 0.5	Hoops	480

Table 2: Mechanical properties of the GFRP reinforcement

Bar type	Nominal diameter mm	Area mm^2	Modulus of elasticity GPa	Tensile strength MPa	Ultimate strain (%)
No. 16	15.9	199[a] (235)[b]	65.7[c]	1,711[d]	2.60[d]
No. 10 (spirals/hoops)	9.5	71[a] (83)[b]	58.4[c]	1,376[d, e]	2.36 [d, e]

[a] Nominal area according to CSA S807-19 [26].
[b] Actual area measured according to Annex A of CSA S806-12 [8].
[c] Calculated according to Annex C of CSA S806-12 [8].
[d] Calculated using nominal area and average force according to Annex C of CSA S806-12 [8].
[e] Determined from tests on straight bars from the same batch as per Annex C of CSA S806-12 [8].

Test Specimens

This study featured casting and testing of three large-scale column-footing connections under simultaneous axial loading and cyclic lateral drift reversals. Two columns had lateral drift reversals applied with a transverse distance, resulting in torsional effects, whereas the third column experienced no torsion as a benchmark. Each connection included a rigid 1,400-mm long and 600-mm deep RC footing, which was adequately reinforced with 15M (16-mm diameter), to provide adequate rotational fixity to the columns during the tests. Each tested column represented the lower portion of a C-bent column, bent in double curvature, between the foundation level and the assumed point of contraflexure.
All columns had a circular cross-section with a 350-mm diameter and shear span equal to 1,750 mm, representing a shear-span-to-depth ratio of 5.0. The design of the test specimens was performed as per CSA S806-12 [8], CSA S6-19 [9], and the findings of the most recent research [1, 6]. All columns were reinforced longitudinally with six No.16 bars and transversely with spirals or hoops at 85-mm pitch [6, 8]. In addition, the lap splice length of the utilized GFRP hoops was 60 times the cross-sectional diameter, as recommended by Abdallah and El-Salakawy [6]. To replicate the common construction practice, the footings were cast first, followed by casting the columns after a week.
A three-character alphanumeric code was used to label the test specimens, where the first letter, G, denoted the GFRP reinforcement used. The second digit represented the torsion-to-bending moment (t_m) ratio, while the last letter indicated the transverse reinforcement configuration (i.e., spiral versus hoops). Table 1 summarizes the details of the tested columns.

Test Setup and Procedure

A horizontal servo-controlled dynamic actuator, with a load and stroke capacities of ±1,000 kN and ± 250 mm, respectively, was used to apply the lateral drift reversals. For specimens G-0.2-S and G-0.2-H, the actuator was attached to a transverse beam, cast monolithically with the column, at a transverse eccentricity, D_i, equal to 350 mm, resulting in a t_m ratio equal to 0.2. The axial loading was applied using a special assembly that comprised of 2000-kN load-capacity hydraulic jack, three unbonded post-tensioned high-strength steel strands, running across a concentric PVC pipe with the column cross-section, and proper end anchorages. The axial load was monitored by a load cell that was attached to the hydraulic jack. A hydraulic pump was connected to the axial loading assembly to maintain a constant axial load on the columns during the test. To provide adequate rotational fixity to the column, the footing was anchored to the laboratory strong floor using high-strength threaded bars. Three draw-wire string potentiometers (SPs) were attached across the transverse beam at the top of each column to measure the lateral drift across the centroid of the column cross-section and to enable the calculation of the twist angle of the columns subjected to torsional effects. The details of the test setup are depicted in Fig. 2.
The first step of the loading protocol was to apply the specified axial load, which was 7.5% of the nominal unconfined axial capacity of the column, P_o, calculated as per CSA S806-12 [8]:

$$P_o = \alpha_1 \phi_c f_c^{'} (A_g - A_F) \quad \text{Eq.1}$$

where α_1 is the ratio of average stress in the rectangular compression stress block to the specified concrete strength (f_c'); ϕ_c is the resistance factor of concrete, assumed herein as unity; A_g is the gross cross-sectional area of the column; and A_F is the total area of the FRP longitudinal reinforcing bars.

(a) Specimen G-0.0-S

(b) Specimens G-0.2-S and G-0.2-H

Fig. 2: Test setup

The following step was to apply the lateral loading, starting with two load-controlled cycles to assess the cracking moment of each column and simulate it at service [2, 4, 6]. Then a displacement-controlled phase was applied with a 0.01-Hz frequency in accordance with ACI 374-05 [27]. Three cycles, with equal drift ratio (i.e., the percentage of the applied lateral displacement to the shear span of the column), were applied for each drift step to promote stable crack progression. Following the applied drift ratio of 2.00%, a load-controlled cycle, with the same peak load as that of the initial service-load cycle, was applied after each drift step to evaluate the stiffness degradation, if any [2, 4, 6, 12-16]. The tests were terminated when the lateral load resistance is below 75% of the peak lateral load accomplished.

EXPERIMENTAL RESULTS AND DISCUSSION

General Observations and Modes of Failure

The cracking load increased as the torsional effects were introduced. As listed in Table 1, the cracking load was 20 kN for G-0.0-S whereas the onset of cracking occurred at a lateral load of 25 kN for G-0.2-S and G-0.2-H. in addition, the cracks initiated in G-0.0-S were horizontal around the circumference of the column section, whereas diagonal cracks were developed in G-0.2-S and G-0.2-H due to the influence of torsion. As the columns underwent the displacement history, more cracks were developed and more cracks propagated diagonally across the column, with higher intensity of the latter in G-0.2-S and G-0.2-H. it was also observed that more extensive cracking occurred for columns G-0.2-S and G-0.2-H over a larger length compared to G-0.0-S. Furthermore, cover spalling occurred earlier for G-0.2-S and G-0.2-H (i.e., at 2.50-% column drift ratio) than for column G-0.0-S (i.e., at a column drift ratio of 3.00%). Such observations agree well with the findings of similar research on steel-RC columns [17-20].

As the drift reversals continued, the column G-0.0-S experienced more cracking until it failed at an average column drift ratio (i.e., average of the values on the pulling and pushing sides) equal to 12.75%, due to concrete core crushing with a flexural inelastic deformability hinge [2] formation above

the column-footing interface, followed by compression failure of the outermost longitudinal bar (Fig. 3a).

(a) G-0.0-S (b) G-0.2-S (c) G-0.2-H

Fig. 3: Test specimens at failure

The cover spalling region for G-0.0-S extended up to 450 mm above the column-footing interface. For specimen G-0.2-S, larger intensity of inclined cracks was observed, with an approximate angle of 55° to the top surface of the footing. More degradation to the concrete core was observed due to the torsional effects, resulting in column failure at an average drift ratio of 8.35% by simultaneous concrete core crushing and compression failure of the outermost longitudinal bar, followed by twisting and shearing of three longitudinal bars on the tension side. The cover spalling region extended for G-0.2-S for an average length of 530 mm above the interface (Fig. 3b). For column G-0.2-H, more severe core degradation was observed since the start of the displacement history, compared to its spiral-confined counterpart. This led to G-0.2-H failing at an average drift ratio of 5.30%, which was significantly lower than the failure drift of G-0.2-S. the failure occurred mainly due to insufficient lap splice length of the used GFRP hoops, which was characterized by the slippage of the lap splice of the hoops at the critical section, accompanied by total core devastation and buckling and delamination of the longitudinal bars, with a limited cover spalling region of 450-mm length (Fig. 3c), indicating localized core damage.

Hysteretic Response

Figure 4 shows the hysteretic responses of the tested specimens, where it can be observed that an additional torque-twist angle response is plotted for columns G-0.2-S and G-0.2-H due to the presence of torsional effects. Narrow hysteresis loops that are aiming towards origin can be observed, which is the characterizing feature for GFRP-RC members due to the linear elastic behavior of GFRP reinforcement [2-6]. In addition, an asymmetric torque-twist response can be observed, which can be attributed to the low t_m ratio applied for those columns [21].

The envelopes of the load-drift and torque-twist hysteretic responses are plotted in Figs. 5a and b, respectively. For the spiral-confined columns (e.g., G-0.0-S and G-0.2-S), higher lateral load resistances and columns drifts can be observed in the pulling direction (i.e., negative sign) than those on the pushing direction (i.e., positive sign), whereas no such effect can be noticed for G-0.2-H. This can be justified by the spiral locking effect on the pulling side which provides better confinement to the concrete core, compared to the pushing side where spiral unlocking effect results in less effective confinement [20].

The lateral loads, torque, drifts and twist angles exhibited by the tested specimens at peak and at failure are listed in Table 3. Applying a t_m ratio of 0.2 resulted in lower lateral load and drift capacity by 25% and 35%, respectively, which agrees well with the results of similar steel-RC columns reported in the literature [20, 28]. The reduction of lateral load and drift capacity was 24% and 48%, respectively, for G-0.2-H compared to G-0.0-S.

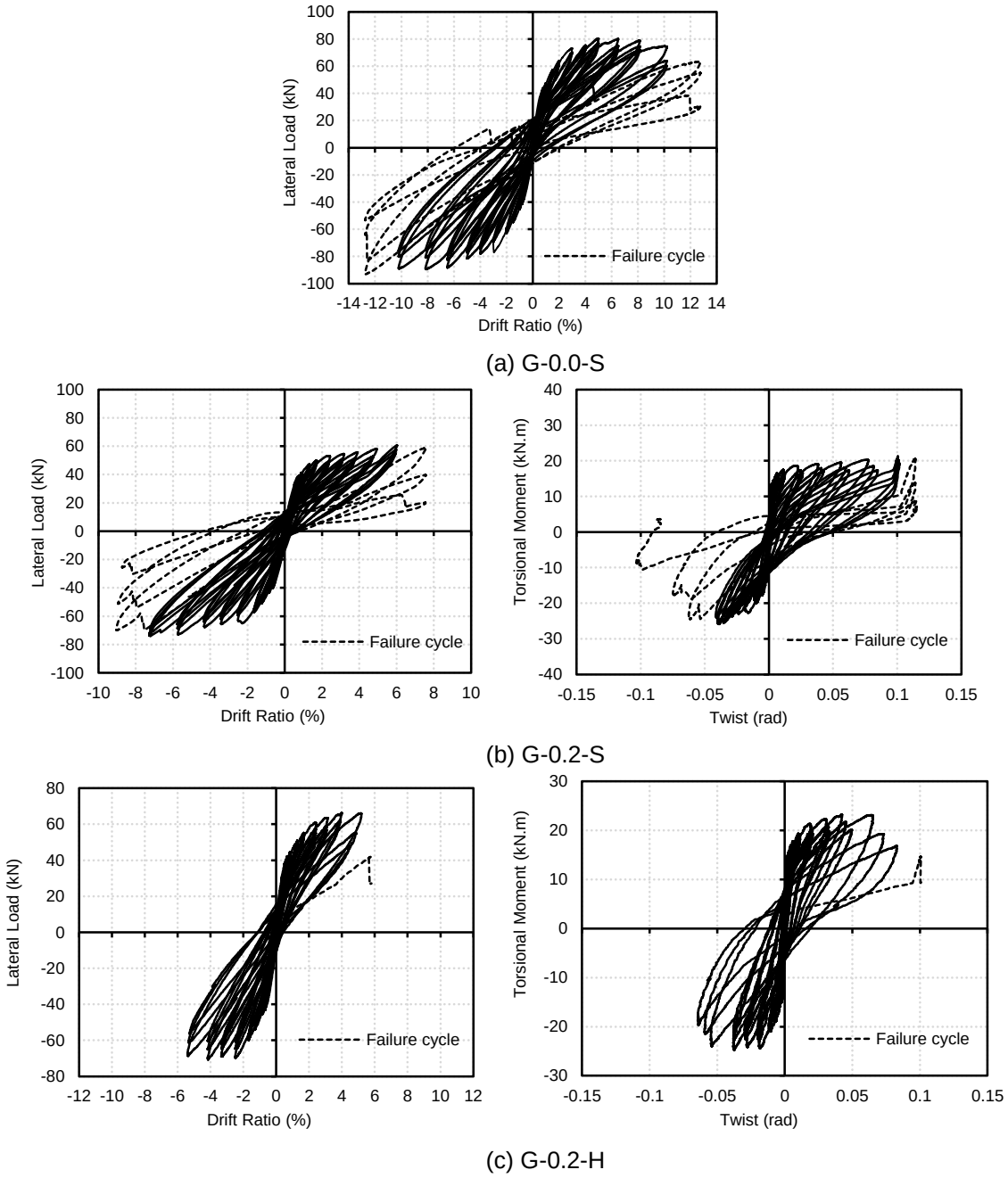

Fig. 4: Hysteretic response of the tested columns

It can be observed that none of the tested parameters affected the initial stiffness of the tested columns. It can also be noticed that all columns exceeded the drift ratio limit of 4.00% set by CSA S806-12 [8] for ductile moment-resistant frame (MRF) structures. However, the failure drift of G-0.2-H was 36% lower than that of its spiral-confined equivalent (i.e., G-0.2-S), which clearly implies the inadequacy of the used GFRP hoops with the lap splice length of 60 d_h recommended by Abdallah and El-Salakawy [6], which exceeds the lap splice length required by CSA S6-19 [9].

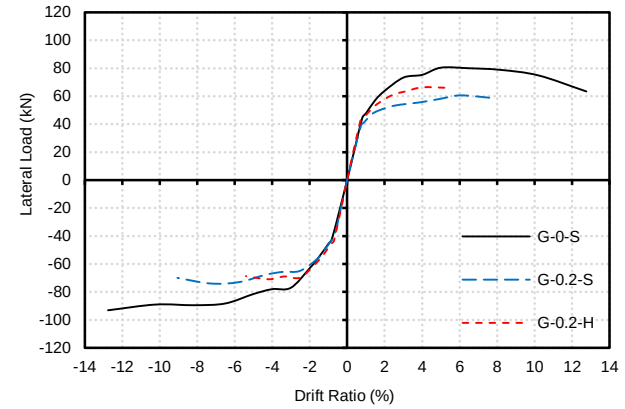

(a)

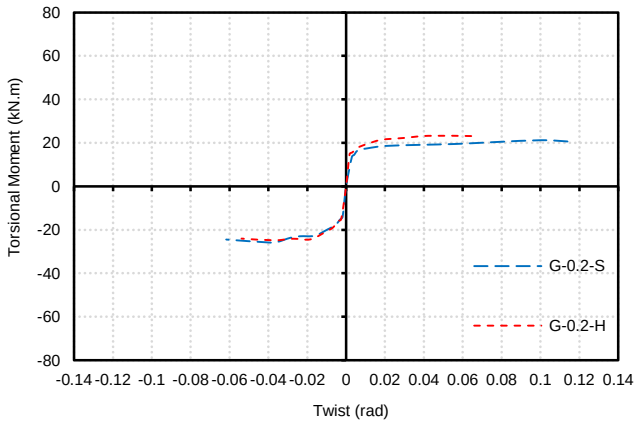

(b)

Fig. 5: Envelopes of the hysteretic responses for the tested columns

Table 3: Experimental results for the tested columns

Specimen ID	Peak lateral load, P_P (kN)		Drift ratio (%)			
	Positive direction (pushing)	Negative direction (pulling)	Positive direction		Negative direction	
			Peak, δ_P	Ultimate, δ_u	Peak, δ_P	Ultimate, δ_u
G-0-S	80.0	89.5	6.50	12.75	8.15	12.75
G-0.2-S	60.6	74.0	6.00	7.60	7.30	9.00
G-0.2-H	66.4	70.9	4.00	5.20	4.20	5.40

CONCLUSIONS

Based on the experimental results of this study, the following conclusions can be drawn:

1. The incorporation of cyclic torsion in C-bent GFRP-RC columns may result in delayed cracking but with higher intensity, earlier cover spalling and larger spalling zone, lower lateral load and drift capacities and more severe mode of failure.
2. The conservative nature of the design equation in Clause 12.7.3.3 of CSA S806-12 [8] for confinement reinforcement of FRP-RC columns in SFRSs can compensate for the detrimental effect that might be caused by torsional effects.
3. Despite being addressed by the available codes [7-9] as a type of confinement reinforcement for FRP-RC columns, the use of discrete circular GFRP hoops, even with the recommended lap splice length of 60 times the hoop cross-sectional diameter [6], may not be allowed for C-

bent columns in seismic areas since they were incapable of providing comparable behavior and capacity to those provided by a spiral-confined column.

ACKNOWLEDGEMENTS

The authors would like to express their gratitude to the Natural Sciences and Engineering Research Council of Canada (NSERC) and the University of Manitoba Graduate Fellowship (UMGF) for their generous financial support. The assistance received from the technical staff at the W. R. McQuade Heavy Structures Laboratory at the University of Manitoba is appreciated.

REFERENCES

1. Tavassoli, A., Liu, J., and Sheikh., S. (2015). “Glass fiber-reinforced polymer-reinforced circular columns under simulated seismic loads.” *ACI Struct. J.* Vol. 112 (1): pp. 103–114.
2. Ali, M. A., and El-Salakawy, E. (2016). “Seismic performance of GFRP-reinforced concrete rectangular columns.” *J. Compos. Constr.* Vol. 20 (3): pp. 04015074.
3. Elshamandy, M. G., Farghaly, A. S., and Benmokrane, B. (2018). “Experimental behavior of glass fiber-reinforced polymer-reinforced concrete columns under lateral cyclic load.” *ACI Struct. J.* Vol. 115 (2): pp. 337–349.
4. Hasaballa, M., and El-Salakawy, E. (2018). “Anchorage performance of GFRP headed and bent bars in beam-column joints subjected to seismic loading.” *J. Compos. Constr.* Vol. 22 (6): pp. 04018060.
5. El-Gendy, M. G., and El-Salakawy, E. F. (2020). “GFRP shear reinforcement for slab-column edge connections subjected to reversed cyclic lateral load.” *J. Compos. Constr.* Vol. 24 (2): pp. 04020003.
6. Abdallah, A. E. M., and El-Salakawy, E. (2021a). “Confinement properties of GFRP-reinforced concrete circular columns under simulated seismic loading.” *J. Compos. Constr.* ASCE, Vol. 25 (2): pp. 04020088.
7. ACI. (2022). “Building Code Requirements for Structural Concrete Reinforced with Glass Fiber-Reinforced Polymer (GFRP) Bars and Commentary.” ACI 440.11-22, *American Concrete Institute,* Detroit. pp. 1–255.
8. CSA. (2017). “Design and construction of building structures with fibre-reinforced polymer.” CSA S806-12 (R2017). *Canadian Standards Association (CSA)*, Toronto, ON.
9. CSA. (2019). “Canadian highway bridge design code.” CSA S6-19." *Canadian Standards Association (CSA)*, Toronto, ON.
10. Kharal, Z., and Sheikh, S. A. (2020). “Seismic behavior of square and circular concrete columns with GFRP reinforcement.” *J. Compos. Constr.* Vol. 24 (1): pp. 04019059.
11. Kharal, Z., Carrette, J. K., and Sheikh, S. A. (2021). “Large concrete columns internally reinforced with GFRP spirals subjected to seismic loads.” *J. Compos. Constr.* Vol. 25 (3), pp. 04021014.
12. Abdallah, A.E., and El-Salakawy, E.F. (2021b). "Seismic Behavior of High-Strength Concrete Circular Columns Reinforced with Glass Fiber-Reinforced Polymer Bars." *ACI Structural Journal*. Vol. 118 (5): pp. 221–34.
13. Abdallah, A.E., and El-Salakawy, E.F. (2022a). "Effect of Aspect Ratio on Seismic Behavior of Glass Fiber-Reinforced Polymer-Reinforced Concrete Columns." *ACI Structural Journal*. Vol. 119 (3): pp. 205–19.
14. Abdallah, A.E., and El-Salakawy, E.F. (2022b). "Seismic Performance of GFRP-RC Circular Columns with Different Aspect Ratios and Concrete Strengths." *Engineering Structures*. Vol. 257 (8): pp. 114092.
15. Abdallah, A.E., Selmy, Y.M., and El-Salakawy, E.F. (2022). "Confinement Characteristics of GFRP-RC Circular Columns under Simulated Earthquake Loading: A Numerical Study." *J. Compos. Constr.* ASCE, Vol. 26 (2): pp. 4022007.
16. Selmy, Y.M., and El-Salakawy, E.F. (2022). "Numerical Investigation on the Seismic Behaviour of GFRP-Reinforced Concrete Rectangular Columns." *Engineering Structures*. Vol. 262 : pp. 114355.
17. Bentz, E.C. (2000). "Sectional Analysis of Reinforced Concrete Members." *Ph.D Thesis* , Department of Civil Engineering, University of Toronto. pp. 316.

18. Otsuka, H., Takeshita, E., Yabuki, W., Wang, Y., Yoshimura, T., and Tsunomoto, M. (2004). "Study on the Seismic Performance Of Reinforced Concrete Columns Subjected to Torsional Moment , Bending Moment and Axial Force." *Proceedings of The13th World Conference on Earthquake Engineering*. Paper No. 393.
19. Belarbi, A., Prakash, S.S., and Silva, P.F. (2010). "Incorporation of Decoupled Damage Index Models in Performance-Based Evaluation of RC Circular and Square Bridge Columns under Combined Loadings." *American Concrete Institute, ACI Special Publication*. (271 SP): pp. 79–102.
20. Prakash, S.S., Li, Q., and Belarbi, A. (2012). "Behavior of Circular and Square Reinforced Concrete Bridge Columns under Combined Loading Including Torsion." *ACI Structural Journal*. Vol. 109 (3): pp. 317–27.
21. Chen, S., Peng, W., and Yan, W. (2018). "Experimental Study on Steel Reinforced Concrete Columns Subjected to Combined Bending–Torsion Cyclic Loading." *Structural Design of Tall and Special Buildings*. Vol. 27 (11): pp. 1–13.
22. Deng, R., Zhou, X.H., Wang, Y.H., Ke, K., Bai, Y.T., Zhu, R.H. and Lei, Z. (2022). "Behaviour of Tapered Concrete-Filled Double-Skin Steel Tubular Columns with Large Hollow Ratio under Combined Compression-Bending-Torsion Loads: Experiments." *Journal of Building Engineering*. Vol. 57 (04): pp. 104876.
23. Prakash, S.S., and Belarbi, A. (2009). "Shear-Flexure-Torsion Interaction Features of Reinforced Concrete Bridge Columns-an Experimental Study." *American Concrete Institute, ACI Special Publication*. (265 SP): pp. 427–53.
24. CSA. (2019). “Concrete materials and methods of concrete construction/test methods and standard practices for concrete.” CSA A23.1-19/A23.2-19. *Canadian Standards Association (CSA)*, Toronto, ON.
25. Pultrall Inc. (2019). “V-ROD—Technical data sheet.” *ADS Comp. Group*. Thetford Mines, QC, Canada.
26. CSA. (2019). “Specification for fibre-reinforced polymers.” CSA S807-19. *Canadian Standards Association (CSA)*, Toronto, ON.
27. ACI. (2019). “Acceptance criteria for moment frames based on structural testing and commentary.” ACI 374.1-05(19). *American Concrete Institute*, Farmington Hills, MI.
28. Ping, C.Z., Su, W., and Yang, Y. (2021). "Seismic Behavior of Reinforced Concrete T-shaped Columns Under Compression-flexure-shear and Torsion Combined Action." *Earthquakes and Structures*. Vol. 20 (4): pp. 431–44.